CHAPTER 3

Results and Discussion

3.1 Copolymerization of methyl methacrylate and styrene.

3.1.1 Infrared results relating to MMA-ST copolymers.

3.1.1 (a) MMA-ST copolymers from free radical copolymerization.

Each of the eight various compositional MMA-ST copolymers were cast in the form of a film from solution in 1,2-dichloroethane and their IR spectra recorded. The eight spectra obtained are presented in Figures 3.1 to 3.8. From these spectra, the presence of ester groups (from MMA) is evident from the carbonyl peak at 5.8 μ m whilst a further sharp but much weaker aromatic band (from ST) appears characteristically at 6.25 μ m.

By now applying a background "tangent-line" technique to the semi-quantitative treatment of the spectial absorbances, an "absorbance ratio" of the methyl methacrylate peak (5.8) μ m) and the styrene peak (6.25), can be computed, such that:

$$\frac{\text{Absorbance at } 5.8\ \mu\text{m}}{\text{Absorbance at } 6.25\ \mu\text{m}} = \frac{\log \frac{P'_o}{P}}{\log \frac{P'_o}{P}}$$

where P_o', P', P_o' and P' are the percent transmittances as shown in Figure 3.2 for each wavelength. After calculation, the results obtained for each copolymer composition were as shown in Table 3.1.

From the experimental results obtained by the method of free radical copolymerization (bulk polymerization), each percentage yield obtained amounted to about 10 %.

From the data in Table 3.1, by plotting the the absorbance ratio :

$$\frac{\text{MMA Absorbance at } 5.8\ \mu\text{m}}{\text{ST Absrobance at } 6.25\ \mu\text{m}}$$

Copolymer composition ratio of MMA-ST (m_1:m_2)	Initial monomer ratio ($[M_1]$: $[M_2]$)	m_1/m_2	Absorbance	$\frac{[M_2]}{[M_1]+[M_2]}$	$\frac{m_2}{m_1 + m_2}$
20 : 80	1.00 : 6.32	0.25	2.53	0.86	0.80
40 : 60	1.00 : 1.72	0.67	4.91	0.63	0.60
50 : 50	1.00 : 0.94	1.00	7.95	0.48	0.50
60 : 40	1.00 : 0.51	1.50	12.77	0.34	0.40
75 : 25	1.00 : 0.20	3.00	22.45	0.17	0.30
80 : 20	1.00 : 0.14	4.00	35.17	0.12	0.20

Table 3.1 Methyl methacrylate-styrene copolymers from free ratical copolymerization together with their infrared absorbance ratios ; ($r_1 = 0.46$, $r_2 = 0.52$, where r_1 and r_2 are the monomer reactivity ratios for MMA and ST respectively).

against the corresponding copolymer composition ratio:-

$$\frac{\text{Methyl methacrylate } (m_1) \text{ in copolymer}}{\text{Styrene } (m_2) \text{ in copolymer}}$$

for each copolymer composition, a straight line graph is obtained as shown in Fig. 3.9.

The linearity of this graph suggests that the peak absorbance of the MMA ester group at 5.8 μm can be taken with some reliance as being directly proportional to both the concentration of MMA in the copolymer. The same can also be said for styrene. Thus, this graph represents a calibration curve for use in analysing the IR spectra obtained by the other various types of copolymerization.

3.1.1 (b) MMA-ST copolymers from anionic copolymerization.

The infrared spectra of the four anionic copolymer products obtained from different monomer compositions (the ratios of the volumes of MMA to those of ST used were 1.0 : 9.0, 3.0 : 7.0, 5.0 : 5.0 and 7.0 : 3.0 ml/ml) were recorded and are shown in Figures 3.11 to 3.14 respectively.

Conversion of these monomer volume ratios of MMA and ST to their corresponding molar ratios (mole/mole) gives:-

From Table 2.5 :- 1 ml. MMA : 9 ml. ST.

MMA 1 ml. = 0.00938 mole.

ST 1 ml. = 0.00871 mole.

$$\text{ST } 9 \text{ ml.} = \frac{0.0087 \times 9}{1} \text{ mole.}$$

$$= 0.0781 \text{ mole.}$$

Thus, the first monomer ratio ($[M_1]$: $[M_2]$) is 1.00 : 8.33 mole/mole. The four monomer concentration ratios are shown in Table 3.2 along with their corresponding copolymer absorbance ratios as calculated from Figures 3.10 to 3.13. Also given are the theoretical copolymer composition values and monomer and polymer styrene fractions.

Volume ratios of MMA-ST (ml/ml)	Initial monomer ratio ($[M_1]:[M_2]$)	Absorbance ratio	Copolymer composition ratio(m_1/m_2)	$\frac{m_2}{m_1+m_2}$	$\frac{[M_2]}{[M_1]+[M_2]}$
1.0 : 9.0	1.00 : 8.33	26.85	2.44	0.29	0.89
3.0 : 7.0	1.00 : 2.17	41.59	3.68	0.21	0.68
5.0 : 5.0	1.00 : 0.93	55.33	5.20	0.16	0.48
7.0 : 3.0	1.00 : 0.40	-	-	-	0.28

Table 3.2 MMA-ST copolymers from anionic copolymerization comparison of absorbance ratios with copolymer and monomer composition data.

The experimental yields obtained from the MMA-ST anionic copolymerizations were much higher than in free radical bulk copolymerization in being at around 50 % in each case.

The IR spectra again show the presence of a very strong ester absorbance peak due to MMA but the aromatic band due to ST is now noticeably weaker than before. This suggests that, in the case of anionic copolymerization using butyl lithium in benzene as initiator, the anionic copolymer chain consists of proportionately more MMA units. Since BuLi is an anionic initiator, its property is consistent with the idea that the metal carbond bond is an intermediate between being covalent, although highly polarized in the direction $Li^{\delta\oplus} \longrightarrow Bu^{\delta\ominus}$, and being fully ionised $Li^{\oplus} + Bu^{\ominus}$. Because the anionic reactivity of MMA towards Buli is much greater than that of ST, as a result of the electron-withdrawing nature of its substituent ester group, the probability of MMA addition to the end of the growing polymer chain is therefore much greater than that for ST. Thus, the experimental serve to confirm that the monomer reactivity ratio, r_1, for MMA is greater than r_2 for ST for anionic copolymerization as shown in Fig. 3.18. Indeed, for a volume ratio of MMA-ST (ml/ml) of 7.0 : 3.0, as shown in Table 3.2, the apparent absence of an aromatic band at 6.25 μm indicates that ST units are either not incorporated into the copolymer chain or, as is more likely, that they are but to such a small extent as not to be sensed by the IR analysis.

3.1.1 (c) MMA-ST copolymers from cationic copolymerization.

The infrared spectra of the four copolymer products obtained from the various monomer compositions are shown in Fig.3.14 to 3.17. The monomer volume ratios of MMA to ST were 1.5 : 3.5, 2.5 : 2.5, 3.5 : 1.5 and 4.0 : 1.0 ml/ml respectively.

Similarly with the previous section 3.11 (b), these volume ratios of MMA and ST are converted into the monomer molar concentration ratios (mole/mole). Also as before, the absorbance ratios from Figures 3.14 to 3.17 are calculated and the results shown in Table 3.3.

Volume ratios of MMA-ST(ml/ml)	Monomer molar concentration ratio ($[M_1]:[M_2]$)	Absorbance ratio	Copolymer composition ratio(m_1/m_2)	$\frac{m_2}{m_1+m_2}$	$\frac{[M_2]}{[M_1]+[M_2]}$
1.5 : 3.5	1.00 : 2.17	0.107	0.10	0.90	0.68
2.5 : 2.5	1.00 : 0.93	0.231	0.23	0.81	0.48
3.5 : 1.5	1.00 : 0.40	0.066	0.067	0.93	0.28
4.0 : 1.0	1.00 : 0.23	0.057	0.06	0.94	0.18

Table 3.3 MMA-ST copolymers from cationic copolymerization ; absorbance ratio and monomer and copolymer composition data.

Since the MMA-ST copolymers obtained from cationic copolymerization prepared at room temperature were of only low molecular weight, they were not able to be film-cast from solution. Consequently, their IR spectra were recorded from KBr discs. However, if the temperature is maintained at very low temperature, in this study at -50°C, copolymers of high molecular weight are obtained from which films can easily be made.

The mechanism of cationic polymerization may be summarized through the following scheme :

Initiation :

$$A + RH \rightleftharpoons A\text{-}RH$$

$$A\text{-}RH + M \longrightarrow HM^{\oplus}\text{---}AR^{\ominus}$$

Propagation :

$$HM^{\oplus}\text{---}AR^{\ominus} + xM \longrightarrow H(M)^{\oplus}_{x+1}\text{------}AR^{\ominus}$$

Termination :

$$HM^{\oplus}_{x+1}\text{---}AR^{\ominus} \longrightarrow M_{x+1} + A\text{-}RH$$

Chain transfer :

$$HM^{\oplus}_{x+1}\text{---}AR^{\ominus} + M \longrightarrow M_{x+1} + HM^{\oplus}\text{------}AR^{\ominus}$$

The relatively low molecular weights of the copolymers obtained can be considered to due to a temperature effect, since the reactions were conducted at room temperature be rather than at the much lower temperatures normally prescribed for cationic polymerization. The reason why low temperatures favour high molecular weight copolymer formation is that the propagation step is favoured over competing reactions resulting from enhanced carbonium in reactivity.

However, the experimental results obtained from cationic copolymerization revealed that high percentage yields (~ 50 %) are nevertheless still obtained as with anionic copolymerization previously.

In contrast to the anionic case, however, the IR spectra for the cationic copolymers show that ester absorbance peak in MMA is now very weak whereas that of the styrene aromatic band is very strong. Thus, this indicates that, in the case of cationic copolymerization using $AlCl_3$ in nitrobenzene as catalyst, a copolymer chain consisting of mainly ST units is produced, i.e., the radical chain shows a tendency to add more ST as opposed to MMA. Because $AlCl_3$ in nitrobenzene, as the cationic initiator, prefers to attack a more electronrich C=C monomer double bond, in this case, that of styrene as opposed to methyl methacrylate, this explains why the observed monomer cationicreactivity ratio, r_1, for MMA is much less than r_2 for ST as shown in Fig.3.18.

The plot of percentage styrene in the monomer feed, ($[M_2]$ /$[M_1]$ + $[M_2]$) against percentage styrene in the copolymer, (m_2/m_1+m_2)is as shown in Fig. 3.18.

From the graph in Fig. 3.18, the monomer reactivity ratio can be determined for the systems using other initiators to these mentioned in the figure, such as Na in liquid ammonia, lewis acid types, ect.

The method involved knowing the monomer concentration feeds of both MMA and ST for various ratios, using Na in liquid NH_3 as the initiator at a given temperature. The copolymers are made into films and their IR spectra are then recorded. The peak absorbance ratios are then measured and used to calibrate the copolymer composition from Fig. 3.9. From the copolymer composition equation (Eq. 4 in Chapter 1), it is possible to calibrate the monomer reactivity ratios (r_1 and r_2) by computer.

3.1.2 Nuclear magnetic resonance results relating to methyl methacrylate-styrene copolymers.

3.1.2 (a) NMR spectra of copolymers from free radical copolymerization.

The proton ^{1}H-NMR spectra of the six methyl methacrylate-styrene free radical copolymers, plus those of the polystyrene and poly (methyl methacrylate) homopolymers, were each recorded and are as shown in Figure 3.19 to 3.26. The resonances of the aryl protons due to ST are seen near 7 ppm whilst the aliphatic resonances from MMA methoxy, methyl, and both MMA and ST main chain protons appear within the relatively wider range below about 3.7 ppm.

From section 2.3 in chapter 2, we have already seen that :

$$\frac{\text{Molar concentration of MMA}}{\text{Molar concentration of ST}} = \frac{5B-3A}{8A}$$

where A is the total area of the aromatic proton resonance at about 7 ppm and B is the total area of all of the remaining aliphatic proton resonances in the copolymer. These areas A and B were each determined from Figures 3.20 to 3.25, corresponding to copolymer compositions of MMA-ST 20 : 80, 40 : 60, 50 : 50, 60 : 40, 75 : 25 and 80 : 20 respectively. However, as can be seen from the NMR spectrum of poly (methyl methacrylate) alone, as shown in Figure 3.26, area A in the copolymer spectra requires correction for the impurity resonance which appears at around 7.4 ppm - arising from $CHCl_3$ impurity in the CCl_4 solvent used.

Thus, the corrected NMR integration area for A reduces slightly to A(x-y)/x

where x = total resonance area over range 6.3 to 7.3 ppm.

and y = resonance area of impurity at 7.4 ppm.

Therefore, the corrected molar concentration ratios of the prepared MMA-ST copolymers can now be determined from the NMR integrations as shown in Table 3.4.

From Table 3.4, each copolymer coposition of MMA-ST obtained from NMR spectral analysis is seen to be less than the theoretical value predicted by the copolymer composition equation. The relation between these two sets of values is as shown in Figure 3.27, the graph obtained being substantially linear, except perhaps for some slight deviation at high MMA/ST molar ratios.

Copolymer composition of MMA-ST ($m_1 : m_2$)	m_1/m_2	A	x	y	corrected A	B	$\frac{5B-3A}{8A}$
20 : 80	0.25	56	9.84	0.73	51.84	43	0.14
40 : 60	0.67	50	8.96	0.61	46.59	69	0.55
50 : 50	1.00	58	4.80	0.20	55.58	108	0.83
60 : 40	1.50	28	2.87	0.45	23.61	62	1.26
75 : 25	3.00	26	2.33	0.47	20.75	105	2.57
80 : 20	4.00	7	1.21	0.15	6.13	41	3.80

Table 3.4 MMA-ST copolymers as obtained from NMR spectral analysis.

Consider now the NMR spectrum of polystyrene alone in Figure 3.19, the resonance areas of the aliphatic protons at 1.5 ppm. and the aryl protons at 6.3-7.3 ppm., which are accurately measurable, are found to be in the ratio of about 3 : 5. This result is therfore, in agreement with the theoretical value calculable for one styrene unit which has three aliphatic protons and five aryl protons. The representation of a styrene unit is as shown below :

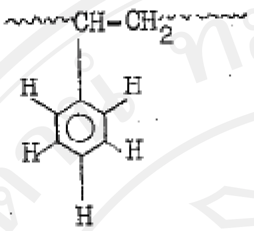

When the various molar concentrations of styrene are copolymerized with methyl methacrylate by free radical copolymerization, yielding copolymers of MMA-ST with composition ratios of 20 : 80, 40 : 60, 50 : 50, 60 : 40, 75 : 25 and 80 : 20, these resonance areas at 1.5 ppm. and 6.3-7.3 ppm., as taken from the NMR integrations for each composition, are found to be in the ratios given in Table 3.5.

Copolymer composition of MMA-ST $(m_1 : m_2)$	m_1/m_2	resonance area at 1.5 ppm.	resonance area at 6.3-7.3 ppm.	$\frac{\text{resonance area at 1.5 ppm.}}{\text{resonance area at 6.3 - 7.3 ppm.}}$
(0 : 100)	(0)	(56)	(98)	(0.6)
20 : 80	0.25	28	46	0.61
40 : 60	0.67	30	38	0.79
50 : 50	1.00	43	48	0.89
60 : 40	1.50	25	23	1.07
75 : 25	3.00	39	22	1.68
80 : 20	4.00	14.5	7	2.07

Table 3.5 The NMR resonance area ratio, as measured for each copolymer coposition of MMA-ST, at 1.5 ppm. and 6.3-7.3 ppm.

From Table 3.5, it can be seen that the resonance area ratio increases as the percentage of MMA in the copolymer increases, this effect obviously being due to the increasing aliphatic resonance contribution, in the the 1.5 ppm. region of the spectrum, from MMA content of the copolymer chain, as represented below:

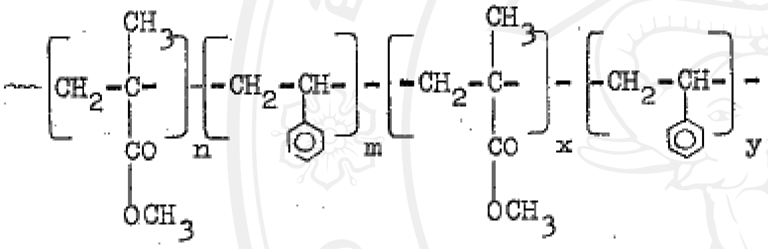

The relationship between the MMA-ST copolymer compositions and their respective 1.5 ppm./6.3-7.3 ppm. resonance area ratios is also found to be linear as shown in Figure 3.28.

3.1.2 (b) <u>NMR spectra of copolymers from anionic copolymerization.</u>

The NMR spectra obtained from copolymers prepared from initial MMA-ST monomer volume ratios (ml/ml) of 7:3, 5:5, 3:7, and 1:9 are as shown in Figures 3.29, 3.30, 3.31 and 3.32 respectively. The spectra show the comparatively weak resonances of the aryl protons, seen near 7.5 ppm., alongside the much stronger , methoxy proton resonances at around 3.7 ppm. On Comparing these spectra with that of poly (methyl methacrylate) homopolymer see Figure 3.26, it is clear that they are very similar in appearance. Consequently, it may be concluded that the anionic copolymer chains consist mainly of MMA rather than ST units - this being consistent with the known preference (i.e., higher reactivity ratio) of MMA over ST for anionic polymerization.

3.1.2 (c) NMR spectra of copolymers from cationic copolymerization.

The NMR spectra obtained from various copolymers, whose initial monomer volume ratios of MMA-ST (ml/ml) were 4:1, 3.5:1.5, 2.5:2.5, and 1.5:3.5 are as shown in Figures 3.33, 3.34, 3.35 and 3.36 respectively. The spectra again show the characteristic proton resonances due to the aryl protons (from ST) and to the aliphatic protons (from MMA and/or ST) in the same relative positions as before.

However, in sharp contrast to the anionic copolymers previously, these cationic MMA-ST copolymers are seen to have much stronger aryl than aliphatic resonances, the spectra being similar in many respects to that of polystyrene alone (see Figure 3.19). Hence, the copolymer chains clearly consist of predominantly styrene as opposed to MMA units, again as would be expected from theory in view of styrene's greater cationic reactivity.

Finally, the NMR spectrum of polystyrene using (a) CCl_4 as a solvent, as shown in Figure 3.19, and (b) deuterochloroform, as shown in Figure 3.37, are seen to be identical and so it can be as assumed that in this case the spectra obtained are not affected by the solvent used.

3.2 Copolymerization of acrylonitrile-styrene.

3.2.1 Preparation by free radical copolymerization.

3.2.1 (a) Introduction.

The free radical copolymerization technique employed in the preparation of acrylonitrile-styrene copolymers was similar to that previously described for the methyl methacrylate-styrene copolymers. Since acrylonitrile can be extremely explosive when heated in air, particular care was taken to ensure that its copolymerizations with styrene were carried out under very carefully controlled temperature conditions under a nitrogen atmosphere.

3.2.1 (b) Experimental details.

In a clean, dry 50 ml. tube were placed 50 mg. of benzoyl peroxide initiator. After deaerating the tube by evacuation and subsequent charging with nitrogen, using a suitable adaptor (see figure 2.4), 50 ml. of the monomer mixture, prepared according to the various compositions given in Table 3.6, were added with a pipette. Then, under a slight excess pressure of nitrogen, the adaptor was replaced with a ground-glass stopper and the tube placed in a thermostat bath at 60°C. After 75 minutes, the contents of the tube were added dropwise and with constant stirring into 500 ml. of methanol. After filtering the copolymer precipitate through a sintered glass filter, the copolymer was then washed with methanol, reprecipitated twice from dimethyl formamide in methanol before being finally dried in vacuo at 60°C.

During copolymerization, the reaction needed to be maintained at 60°C or less for resons of safety and conducted in a controlled inert atomosphere such as nitrogen. From the experimental results obtained from free radical copolymerization (bulk polymerization), percentage yields

Copolymer composition of ACN-ST (m_1 : m_2)	Volume of ACN used (ml)	Volume of ST used (ml)	Time of copolymerization (mins)
0 : 100	-	50	75
20 : 80	3.60	46.40	75
25 : 75	5.20	44.80	75
40 : 60	14.97	35.03	75
50 : 50	32.45	17.55	75
60 : 40	44.55	5.45	75
75 : 25	48.32	1.68	75
80 : 20	48.89	1.11	75
100 : 0	50	-	75

Table 3.6 Compositions of initial monomer mixtures of ACN-ST and time of copolymerization ; $r_1 = 0.04$, $r_2 = 0.41$ (where r_1 is the reactivity ratio of ACN and r_2 is the reactivity ratio of ST at 60°C)

of around 10 % were obtained. Hoever, this figure tended to increase slightly as the mole fraction of ACN in the initial monomer feed increased.

3.2.2 IR data relating to the acrylonitrile-styrene copolymers.

Films for IR analysis of the first six ACN-ST copolymer compositions (0:100, 20:80, 25:75, 40:60, 50:50 and 60:40) were cast from solution in 1, 2-dichloroethane whilst the three remaining compositions (75:25, 80:20 and 100:0) were film-cast from dimethyl formamide. The IR spectra which were subsequently recorded are shown in Figures 3.38 to 3.46. From these spectra, it can be seen that whilst the major features arise initially from styrene, the presence of acrylonitrile becomes increasingly evident in the later spectra through its characteristic C≡N peaks (See figure 3.46). In addition, the absorbance ratioing of characteristic spectral peaks, in this case those at 4.4 μ m and 6.25 μ m due to acrylonitrile and styrene respectively, again appears to be a satisfactory method of semi-quantitatively estimating the relative composition of the copolymers ; that is :

$$\frac{\text{ACN absorbance at } 4.4\ \mu\text{m}}{\text{ST absorbance at } 6.25\ \mu\text{m}} = \frac{\log \frac{P_o}{P}}{\log \frac{P'_o}{P'}} \propto \frac{m_1}{m_2}$$

where P_o, P, P'_o and P' are all percent transmittances as measured at the appropriate of these two wavelengths. After calculation, the results obtained for each copolymer composition are as shown in Table 3.7.

From the data in Table 3.7, it is note that the last two ACN-ST copolymer compositions of 75:25 and 80:20 fail to exhibit in their respective IR spectra (See Figures 3.44 and 3.45) any discernable absorbance peak at 6.25 μ m for ST. Their absorbance ratios are, therefore, not able to be determined for inclusion into Table 3.7.

In possible explanation of this, it is perhaps worth noting that, commercially, ACN-ST copolymers generally contain no more than 20-30 % ACN. There is a possibility that, in the case of the last two copolymers prepared here, the questionable compatibility of such a small volume of styrene in such a relatively large excess of the more polar ACN co-monomer could have resulted in the ST failing to become incroporated to a spectroscopically measurnble extent in the copolymer. Additionally, if the ST were to have preferred to homopolymerize with itself in such small amounts, the polystyrene monomer so produced would doubtlessly have been of such low molecular weight as to have removed during the precipitation and/or washing process.

Copolymer composition of ACN-ST (m_1 : m_2)	monomer ratio (M_1 : M_2)	m_1/m_2	Absorbance ratio $\left(\frac{A_{ACN}}{A_{ST}}\right)$	$\frac{M_2}{M_1 + M_2}$	$\frac{m_2}{m_1 + m_2}$
20 : 80	1.00:7.37	0.25	0.55	0.88	0.80
25 : 75	1.00:4.94	0.33	0.84	0.83	0.75
40 : 60	1.00:1.34	0.67	1.39	0.57	0.60
50 : 50	1.00:0.31	1.00	2.24	0.24	0.50
60 : 40	1.00:0.07	1.50	3.27	0.06	0.40
75 : 25	1.00:0.02	3.00	-	0.02	0.03
80 : 20	1.00:0.013	4.00	-	0.01	0.20

Table 3.7 Acrylonitrile-styrene copolymers from free radical copolymerization ; absorbance ratios together with monomer and copolymer composition data.

On plotting the ratio

$$\frac{\text{ACN absorbance at } 4.4\ \mu\text{m}}{\text{ST absorbance at } 6.25\,\mu\text{m}}$$

against the corresponding copolymer composition ratio

$$\frac{\text{Acrylonitrile } (m_1)}{\text{Styrene } (m_2)}$$

for all copolymer compositions except the last two given in Table 3.7, an apparent straight line relationship of the form shown in Figure 3.47 is found.

This absorbance ratio graph thus constitutes a calibration curve which can be usefully employed in estimating copolymer composition from IR absorbance data for those copolymerization types for which the individual monomer reactivity ratios may not be known so accurately.

Also from the data in Table 3.7, on plotting the mole fraction of styrene in the monomer feed

$$\frac{[M_2]}{[M_1] + [M_2]}$$

against the styrene fraction contained in the copolymer (m_2/m_1+m_2), the curve shown in Figure 3.48 is obtained.

A final note worth mentioning here is that whilst ACN undergoes free radical polymerization, its electron deficient C=C double bond, arising from the strong electron-withdrawing nature of the -C≡N group, lends itself much more to anionic polymerization.

Conversely, ACN does not undergo cationic polymerization to any worthwhile extent.

3.2.3 NMR results relating to acrylonitrile-styrene copolymers.

The NMR spectra of the seven prepared free radical copolymers of ACN-ST, corresponding to calculated copolymer composition equation ratios of 20:80, 25:75, 40:60, 50:50, 60:40, 75:25 and 80:20, together with that of polyacrylonitrile homopolymer, were recorded and are as shown in Figures 3.49, 3.50, 3.51, 3.52, 3.53, 3.54, 3.55 and 3.56 respectively.

The first four of these copolymer spectra each exhibit resonances in the region of 1.6 ppm. and 6.5-7.6 ppm., whilst the remaining three, plus that of polyacrylonitrile, show little or no NMR response-ostensibly due to their apparent insolubility in the deuterochloroform solvent. However, the 1.6 ppm. /6.5-7.6 ppm. resonance area ratios, wherever possible, were calculated and are given in Table 3.8 for their respective copolymer compositions.

Copolymer composition of ACN-ST (m_1 : m_2)	m_1/m_2	NMR resonance area at 1.6 ppm.	NMR resonance area over range 6.5-7.6 ppm.	resonance area at 1.6 ppm. / resonance area from 6.5-7.6 ppm.
20 : 80	0.25	28	48	0.58
25 : 75	0.33	34	46	0.74
40 : 60	0.67	37	43	0.86
50 : 50	1.00	58	41	1.41
60 : 40	1.50	-	-	-
75 : 25	3.00	-	-	-
80 : 20	4.00	-	-	-

Table 3.8 The NMR resonance area ratio, as measured for each copolymer composition of ACN-ST, at 1.6 ppm. and 6.5-7.6 ppm.

From Table 3.8, it can be seen that the resonance area ratios for the 20:80, 25:75, 40:60 and 50:50 ACN-ST copolymers, which, incidentally dissolved satisfactorily in the $CDCl_3$ solvent, increase from 0.58 to 1.41 as the proportion of ACN in the copolymer increases. This change undoubtedly reflects the increasing appearance in the copolymer of aliphatic methylene protons due to ACN units-the initial ratio of 0.58 confirming the expected aliphatic/aryl proton ratio of 0.6 corresponding to a copolymer largely consisting of ST blocks.

Regrettably, however, the solubility difficulties encountered with the more ACN- rich copolymers precludes their further study. However, for those copolymers which could be dissolved, their resonance area ratios, plotted as a function of composition, are shown in Figure 3.57. The non-linearity of the graph, contrasting as it does with that found for the MMA-ST copolymers, previously, probably reflects the more complicated "copolymer composition with respect to solubility" situation which we have here.